Triosephosphate Isomerase: A Theoretical Comparison of Alternative Pathways

Qiang Cui[†] and Martin Karplus*[,†,‡]

Contribution from the Department of Chemistry and Chemical Biology, Harvard University, Cambridge, Massachusetts 02138, Laboratoire de Chimie Biophysique, ISIS, Université Louis Pasteur, 67000 Strasbourg France

Received August 4, 2000. Revised Manuscript Received December 27, 2000

Abstract: Three mechanisms proposed for the triosephosphate isomerase (TIM) catalyzed reactions were studied with the QM/MM approach using B3LYP/6-31+G(d,p) as the QM method. The two pathways that involve an enediol species were found to give similar values for the barriers and the calculated rates are in satisfactory agreement with experiment. By contrast, the mechanism that involves intramolecular proton transfer in the enediolate was found to be energetically unfavorable due to electrostatic interactions with His 95, a conserved residue in TIM from different organisms. A perturbation analysis was used to determine the residues that make the major contribution to catalysis.

Introduction

Triosephosphate isomerase (TIM) is a dimeric enzyme that catalyzes the conversion of dihydroxyacetone phosphate (DHAP) and glyceraldehyde 3-phosphate (GAP), an important step in the glycolytic pathway.[1] It has been referred to as a "perfect enzyme" because the chemical steps of the reaction are accelerated sufficiently so that the diffusion steps are rate-limiting.[2] Despite numerous experimental[2−6] and theoretical studies,[7−10] the precise chemical mechanism of the multistep reaction catalyzed by TIM is not fully elucidated (see Scheme 1). The observed proton exchange between solvent and the enzyme with bound substrate suggested that an intermediate is involved in the catalyzed reaction,[2] although there may be more than one; the identity of the intermediate(s) is not clear from experiments. There is agreement on the first step (transfer of a proton from DHAP to Glu 165 to form an enediolate) and the last step (transfer of a proton from GluH 165 to an enediolate to form GAP), but there are three alternative proposals for the intermediate step (transfer of a proton from O_1 of the enediolate EDT1 to O_2 so as to form EDT2), and there is some support for each possibility; for a recent analysis see Mildvan et al.[4b,c] (see below). Two pathways (paths A and C in Scheme 1) involve generation of an enediol (EDL), either by transfer of a proton from and to His 95 (path A) or by transfer of a proton from and to GluH 165 (path C). The third proposal (path B) involves internal proton transfer from O_1 to O_2 without formation of an enediol.

Path A was proposed by Knowles and co-workers.[2] Although it is based on a range of experiments, there is no *direct* evidence for intermediate formation of an *enediol* during the reaction. Nevertheless, the mechanism has been widely accepted. Due to the fact the TIM-catalyzed reactions are in the diffusion limit, direct evaluation of the reaction free energy from kinetic measurement is not possible. The experimental estimates were obtained by use of the elegant isotope exchange−conversion technique;[2] kinetic measurements with isotope-labeled substrate in ^1H_2O and unlabeled substrate in tritiated water were analyzed to yield the free energy profiles of the significant kinetic steps. The energetics related to path A have been analyzed theoretically and supported by Bash et al.[7] with QM/MM calculations at the AM1/CHARMM level. A major conclusion from that work is that the general acid involved in the catalysis is a *neutral* histidine (His 95), which was later verified experimentally using NMR spectroscopy.[4a] The mechanism was also supported by the detailed study of Åqvist and Fothergill[8] with an EVB model using a free energy perturbation technique. One active-site water molecule and certain residues from the other subunit were found to be important, although no quantitative evaluation of their effect was given.

Algona et al.[9] proposed an alternative mechanism (path B), in which an intramolecular proton transfer leads from EDT1 to

[†] Harvard University.
[‡] Université Louis Pasteur.

(1) For a review, see Knowles, J. R. *Nature*, **1991**, *350*, 121.
(2) (a) Herlihy, J. M.; Maister, S. G.; Albery, W. J.; Knowles, J. R. *Biochemistry* **1976**, *15*, 5607 (b) Albery, W. J.; Knowles, J. R. *Biochemistry* **1976**, *15*, 5627 (c) Albery, W. J.; Knowles, J. R. *Biochemistry* **1976**, *15*, 5588 (d) Knowles, J. R.; Albery, W. J. *Acc. Chem. Res.* **1977**, *10*, 105.
(3) (a) Davenport, R. C.; Bash, P. A.; Seaton, B. A.; Karplus, M.; Petsko, G. A.; Ringe, D. *Biochemistry* **1990**, *30*, 5821 (b) Lolis, E.; Alber, T.; Davenport, R. C.; Rose, D.; Hartman, F. C.; Petsko, G. A. *Biochemistry* **1990**, *29*, 6609.
(4) (a) Lodi, P. J.; Knowles, J. R. *Biochemistry* **1991**, *30*, 6948 (b) Harris, T. K.; Abeygunawardana, C.; Mildvan, A. S. *Biochemistry* **1997**, *36*, 14661 (c) Harris, T. K.; Cole, R. N.; Comer, F. I.; Mildvan, A. S. *Biochemistry* **1998**, *37*, 16828.
(5) (a) Belasco, J. G.; Knowles, J. R. *Biochemistry* **1980**, *19*, 472 (b) Komives, E. A.; Chang, L. C.; Lolis, E.; Tilton, R. F.; Petsko, G. A.; Knowles, J. R. *Biochemistry* **1991**, *30*, 3011
(6) (a) Nickbarg, E. B.; Davenport, R. C.; Petsko, G. A.; Knowles, J. R. *Biochemistry* **1988**, *27*, 5948 (b) Pompliano, D. L.; Peyman, A.; Knowles, J. R. *Biochemistry* **1990**, *29*, 3186 (c) Zhang, Z.; Komives, E. A.; Sugio, S.; Blacklow, S. C.; Narayana, N.; Xuong, N. H.; Stock, A. M.; Petsko, G. A.; Ringe, D. *Biochemistry* **1999**, *38*, 4389.
(7) Bash, P. A.; Field, M. J.; Davenport, R. C.; Petsko, G. A.; Ringe, D.; Karplus, M. *Biochemistry* **1991**, *30*, 5826.
(8) Åqvist, J.; Fothergill, M. *J. Bol. Chem.* **1996**, *271*, 10010; this paper gives an insightful review of earlier theoretical work.
(9) (a) Alagona, G.; Desmeules, P.; Ghio, C.; Kollman, P. A. *J. Am. Chem. Soc*. **1984**, *106*, 3623 (b) Alagona, G.; Ghio, C.; Kollman, P. A. *J. Mol. Biol*. **1986**, *191*, 23 (c) Alagona, G.; Ghio, C.; Kollman, P. A. *J. Am. Chem. Soc.* **1995**, *117*, 9855.
(10) (a) Peräkylä, M. *J. Chem. Soc., Perkin Trans*. **1997**, 2185 (b) Peräkylä, M.; Pakkanen, T. A. *Proteins* **1996**, *25*, 225.

10.1021/ja002886c CCC: $20.00
Published on Web 02/14/2001

Scheme 1. Proposed Catalytic Mechanisms for TIM-Catalyzed Reactions

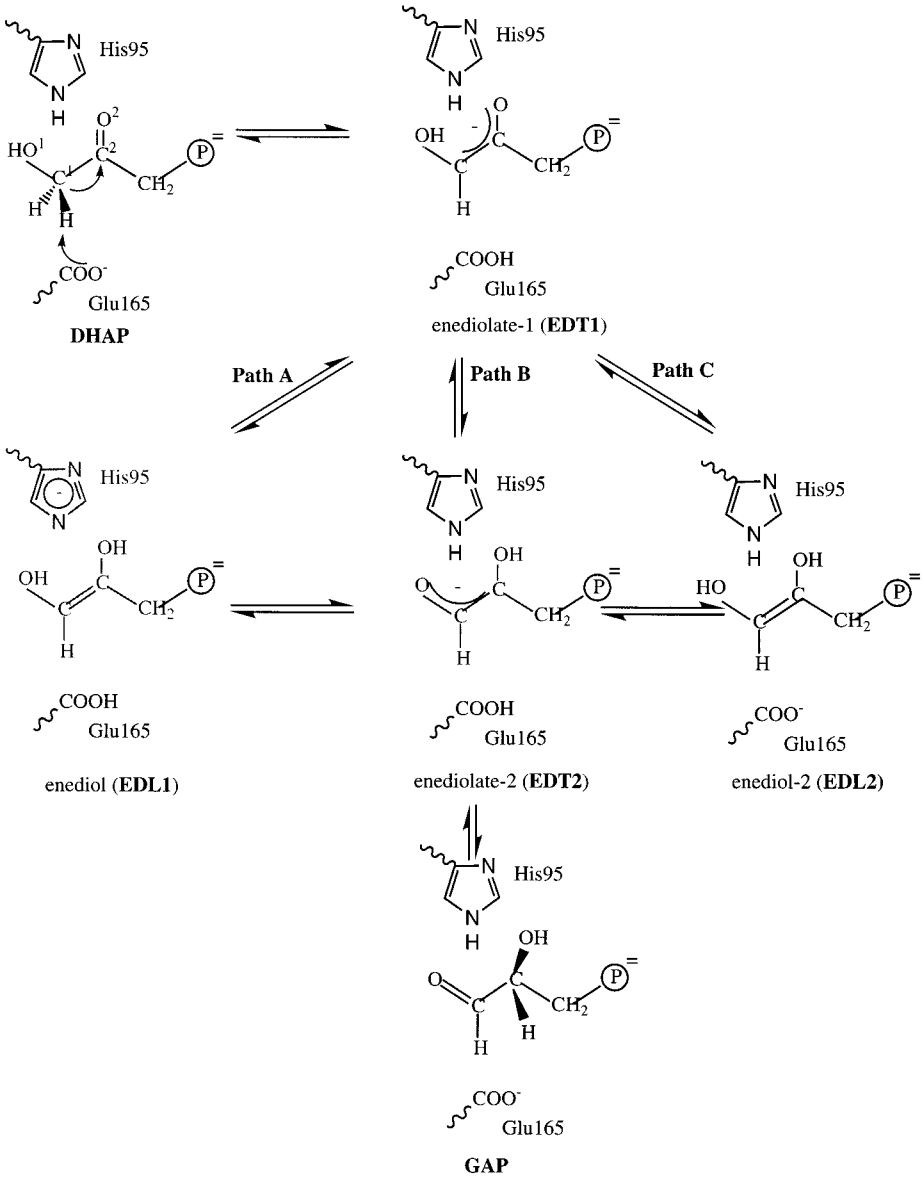

EDT2 without proton transfer from His 95. With a simplified model of the enzyme active site and a QM/MM type approach at the MP2/3-21+G level, they obtained a barrier of 12 kcal/mol for the intramolecular transfer and found that path A involved an endothermic process requiring about 20 kcal/mol. The latter result differs drastically from the work of Bash et al.[7] and Aquist and Fothergill,[8] as well as from the present calculations (see below). Although the origin of this difference is not clear, Algona et al.[9] emphasize "that our [their] model for representing the environment is not quantitatively reliable".

The third mechanism, path C in Scheme 1, has been discussed by a number of authors.[4b,c,6,10] In this path, Glu 165 is the only catalytic residue; it transfers protons during the reaction as shown in Scheme 1. According to the X-ray structure of wild-type TIM with bound PGH,[3] a large displacement of the Glu 165 side chain is necessary in path C, while the position of His 95 is ideal for the proton transfers proposed in path A. Consequently, this mechanism was proposed by Knowles et al.[6] only for TIM in the absence of His 95, that is, in the His95Q mutant, where the rate is reduced by 200-fold[5b,6a] and Glu 165 is in a somewhat worse position to pick up the proton from DHAP.[5b]

Recently Harris et al.[4b,c] carried out NMR experiments on yeast TIM and observed a strongly deshielded proton at 14.9 ppm in the enzyme with the inhibitor PGH in the active site. It is 6.2 ppm downfield relative to free PGH in solution, which suggests that there is a strong hydrogen bond between the carboxylate of Glu 165 and the N−OH proton of PGH. On the basis of this observation and measured exchange rate of the His 95 Nϵ proton with solvent, they proposed that path C may take place in the wild-type enzyme as well. In a set of isotope experiments,[4c] the extent of tritium transfer from the *pro*-R position in DHAP to GAP was studied as a function of substrate concentration. Analysis of the results suggests that the "classical" mechanism (path A) contributes at least 3.9% in yeast TIM. The partition between paths A and C was impossible to estimate because of the uncertainty in the efficiency of conservation and transfer of tritium in the enzyme active site. Path B was not discussed by the authors of refs 4b,c, although one expects an isotope transfer similar to that of path A. Therefore, the experiments in refs 4b,c do not rule out path A or B and do not support path C. Prior to these experiments, Peräkylä et al.[10] had analyzed the mechanism of the TIM-catalyzed reaction in a series of ab initio calculations on model systems with emphasis

on path C. They found that EDL2 is more stable than EDL1, which occurs in path A, so that they speculated that path C is more likely. However, saddle points were not located in their study, and the model was limited to the substrate, Glu 165, His 95, Asn 10, and Lys 12; the environmental effect was described with the finite difference Poisson−Boltzmann method. No calculation was performed to explain the observed importance of His 95 for the catalysis.

In this work, we present QM/MM calculations for the three alternative pathways in the enzyme, as well as for the initial and final chemical steps. They were performed in a consistent manner with a high enough QM level (B3LYP[11] with a 6-31G+-(d,p) basis set[12]) to obtain meaningful results. Computational details are summarized in Sections II, and Section III presents the Results and Discussion. The conclusions concerning the contribution of the three pathways in the enzyme are presented in Section IV. A more detailed description of the structures involved in the various steps of the enzymatic reaction and the energetics of the catalysis, as well as comparisons with related reactions in the gas phase and solution, are presented in a separate publication (to be submitted).

Computational Methods

In the current work, the three pathways were analyzed using the QM/MM calculations at the level of B3LYP[11] associated with a 6-31G+(d,p) basis set.[12] Test calculations on related model systems with high-level ab initio methods, including MP2 and CCSD with a 6-311+G(d,p) basis set, demonstrate that the B3LYP approach with the present basis set is sufficient for calculating reliable activation barriers (see Supporting Information). The program CHARMM[13] interfaced with CADPAC[14,15] was employed for the calculations. Structures were optimized with a smaller QM region that includes only the substrate and the catalytic residue (Glu 165 *or* His 95) explicitly involved in a given proton-transfer step. Link atoms were introduced between the Cα and Cβ atoms in the QM side chain to saturate the valence of the Cβ boundary QM atom. The link atoms interact with the MM atoms, except the "link host" MM atom (the Cα atom in this case), through electrostatic terms; no van der Waals interactions are included. This scheme has been shown to be a satisfactory way to treat the QM/MM interface, particularly when the charges of the atom in the neighborhood of the link atom are small;[16] this is true in the present case. Energetics were obtained from single point B3LYP/6-31+G(d,p)/CHARMM calculations with a QM region that includes the substrate and the side chains of Glu 165 *and* His 95 with the indicated partitioning. Each reaction (see Scheme 1) was followed by using $\mathbf{s} = (\mathbf{r}_{D-H} - \mathbf{r}_{A-H})$ as the reaction coordinates, where D and A are the proton donor and acceptor, respectively. To determine the transition state, adiabatic mapping[17] as a function of **s** was performed for each step. The comparison of the various paths is simplified by the fact that a proton is being transferred (i.e., not liberated or absorbed) in all cases. Test calculations using a simpler QM method at the AM1-SRP/CHARMM level suggest that adiabatic mapping (rather than stringent saddle point optimization) is sufficient for the current purpose. AM1-SRP (SRP denotes "specific reaction parameters"[18]) is a modified version of AM1 with a set of AM1 parameters (i.e., parameters for C, O, H, and N atoms) optimized for the TIM reactions based on B3LYP/6-31+G(d,p) gas-phase results for model systems. The minimized structures and energies were also found to be similar to the potentials of mean force calculated for several proton-transfer steps at the AM1-SRP/CHARMM level; the optimized AM1 parameters and details of the results will be given separately.

As the starting structure, the 1.8 Å resolution X-ray structure of the yeast TIM−PGH complex[3a] was used with the HNOH group of PGH replaced by H_2COH of DHAP; the rms difference from the X-ray structure of the heavy atoms in the active region of the stochastic boundary system was 0.35 Å (0.50 Å) for the mainchain (all heavy atoms) after minimization. A stochastic boundary treatment of the active site in one of the subunits (some residues, particularly Thr75, of the other subunit were included and contribute to the catalysis) was used, and Poisson−Boltzmann charge scaling[19] was introduced to account for solvent shielding in addition to that from the explicit water molecules[20] in the model. The algorithm makes use of several Poisson−Boltzmann calculations to determine a set of scaling factors (shown in Supporting Information) to reduce the partial charges of charged side chains in the QM/MM calculations so as to avoid artifactual structural changes.[19] After the simulations are completed, another set of Poisson−Boltzmann calculations is carried out to correct for the charge scaling and include solvation effects for the fully charged system.[19] Calculations at the AM1/CHARMM level made to compare with the results of Bash et al.,[7] who did not include solvent shielding, showed that the charge-scaling scheme stabilizes the EDL1 and GAP by 4−5 kcal/mol; the relative energetics of other steps are not greatly affected. Given the B3LYP results for the energies, vibration corrections for the stationary points (minima and transition states) along the reaction path were introduced by using AM1/SRP and a model including 450 atoms.

To analyze the effects of individual amino acid residues on the reaction energetics, a perturbational treatment similar to that used in ref 7 was performed. Due to the large number of QM/MM calculations that are required, the analysis was carried out at the AM1-SRP/CHARMM level, which was found to give semiquantitative results as compared to B3LYP/CHARMM calculations.

Because of the multiple steps in the chemical reactions, as shown in the Scheme, kinetic modeling was performed with the calculated activation free energies to determine the contributions of the different pathways. Both the exact analytic solutions[21] and steady-state approximations were used for the coupled unimolecular reactions in the enzyme; the bimolecular steps involving binding of substrate and release of product were not considered since they do not affect the relative contributions of the three paths. To determine the rate constants for each elementary step, transition-state theory (TST) was used with vibrational free energies calculated with the QM/MM method[22] for each stable species and transition state; the free energies relative to EDT1 are listed in parentheses in Figure 1. The corrections to TST rate constants due to the effects of recrossing and proton tunneling were not included in the present analysis. However, the effects are small, relative to those of the lowering of the transition-state barriers by the enzyme (ref 23 and to be published).

Results and Discussions

Energetics of Different Pathways. Figure 1 shows the energy results for the stable species and transition-state barriers along the three different paths; EDT1, which is common to all

(11) (a) Becke, A. D. *Phys. Rev. A* **1998**, *38*, 3098 (b) Lee, C.; Yang, W.; Parr, R. G. *Phys. Rev. B* **1988**, *37*, 785 (c) Becke, A. D. *J. Chem. Phys*. **1993**, *98*, 5648.

(12) (a) Ditchfield, R.; Hehre, W. J.; Pople, J. A. *J. Chem. Phys*. **1971**, *54*, 724 (b) Hehre, W. J.; Ditchfield, R.; Pople, J. A. *J. Chem. Phys*. **1972**, *56*, 2257 (c) Hariharan, P. C.; Pople, J. A. *Theor. Chim. Acta*. **1973**, *28*, 213.

(13) Brooks, B. R.; Bruccoleri, R. E.; Olafson, B. D.; States, D. J.; Swaminathan, S.; Karplus, M. *J. Comput. Chem*. **1983**, *4*, 187.

(14) CADPAC 6.0: The Cambridge Analytical Derivatives PACage, Amos, R. D. et al. Cambridge University, U. K. 1995.

(15) Lyne, P. D.; Hodoscek, M.; Karplus, M. *J. Phys. Chem. A* **1998**, *103*, 3462.

(16) Reuter, N.; Dejaegere, A.; Maigret, B.; Karplus, M. *J. Phys. Chem. B* **2000**, *104*, 1720.

(17) Brooks, C. L., III, Karplus, M.; Pettitt, B. M. *Proteins, A theoretical perspective of dynamics, structure and thermodynamics*; Advances in Chemical Physics, Vol. LXXI; John Wiley & Sons: New York, 1988; p 123.

(18) Gonzalez-Lafont, A.; Truong, T. N.; Truhlar, D. G. *J. Phys. Chem*. **1991**, *95*, 4618.

(19) Simonson, T.; Archontis, G.; Karplus, M. *J. Phys. Chem. B* **1997**, *101*, 8349.

(20) Neria, E.; Fischer, S.; Karplus, M. *J. Chem. Phys*. **1996**, *105*, 1902.

(21) Bashford, D.; Cohen, F. E.; Karplus, M.; Kuntz, I. D.; Weaver, D. L. *Proteins*, **1988**, *4*, 211.

(22) Cui, Q.; Karplus, M. *J. Chem. Phys*. **2000**, *112*, 1133.

(23) (a) Neria, E.; Karplus, M. *Chem. Phys. Lett*. **1997**, *267*, 23 (b) Neria, E.; Karplus, M. *J. Chem. Phys.* **1996**, *105*, 10812.

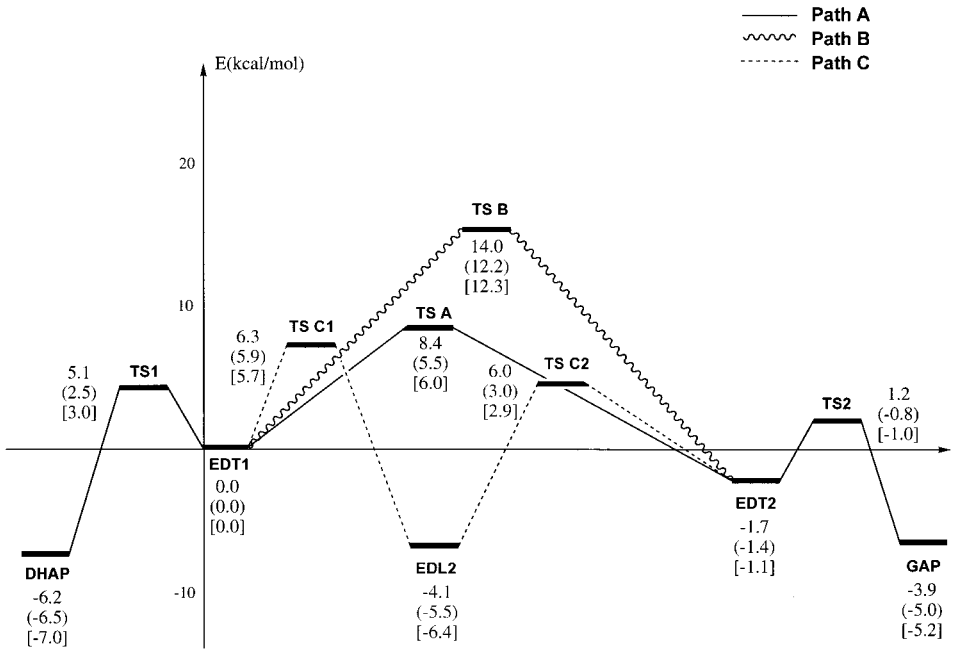

Figure 1. Schematic potential energy profiles for different paths in the TIM reactions from QM/MM calculations. Numbers are obtained from single-point B3LYP/6-31+G(d,p)/CHARMM calculations with a QM partition that includes the substrate, Glu 165 *and* His 95, at the structures optimized with a smaller QM region that includes only the substrate and the catalytic residue (Glu 165 *or* His 95) explicitly involved in a given proton-transfer step. The values in the parentheses include zero-point corrections, and the values in the brackets are effective free energies obtained by adding vibrational free energy contributions (see Methods). The absolute energy for the reference structure EDT1 is −1445.91678 hartree, the zero-point correction is 3.64467 hartree, and the vibrational free energy is 3.44308 hartree. The dominant contribution that lowers the transition-state free energy, relative to the stable states, comes from the zero-point correction. The correction is larger for TSC2, the transition state between EDL2 and EDT2 along path C, because EDL2 has somewhat smaller vibrational contributions compared to EDT1; most of the difference originates from modes with frequencies below 1000 cm^{-1}.

paths (see Scheme 1), is used as the zero of energy. The intramolecular proton transfer (path B) has a significantly higher barrier between EDT1 and EDT2 (14.0 kcal/mol) than either intermolecular path. Analysis of the contribution to the energies by a perturbation method[7] (see below) indicates that His 95 destabilizes the intramolecular transition state by about 5 kcal/mol; this is in agreement with the calculations of Alagona et al.[9c] as cited by Åqvist and Fothergill.[8] Model calculations suggest that the transition state is significantly lower in the H95Q mutant[6a] so that the intramolecular path may contribute in this case (see below). The two intermolecular proton transfer paths have similar calculated activated energies, although path C is more complex structurally because a displacement of Glu 165 is required to permit it to transfer a proton to O_2 of EDT1 (to form the enediol EDL2) and to pick up a proton from O_1 (to form EDT2); Glu 165 moves by 0.90 Å (rms displacements for all heavy atoms in Glu 165) to reach the transition state for the reaction. The stability of EDL2 along path C and the lack of stability of EDL1 along path A is due to the difference in the deprotonation energy of GluH 165 and His 95.[24]

Perturbation Analysis of Electrostatic Contributions. The electrostatic terms make the dominant contribution to the relative stability of the stationary points; van der Waals terms are small in the minimized structures. Consequently, the perturbation analysis is restricted to the former. For the intramolecular proton transfer mechanism (path B), which has the highest barrier among the three pathways, His 95 has the dominant effect and increases the barrier height by nearly 5 kcal/mol (Figure 2a); Lys 12 and the mainchain of Glu 209, as well as W28, make significant contributions.Since the unfavorable effect from His 95 is electrostatic and not steric in nature, the possible structural displacements of His 95 do not alter the barrier significantly. Indeed, potential of mean force calculations at the AM1-SRP/CHARMM level found a free energy barrier very similar to that obtained here. To further investigate the destabilizing effect of His 95 in path B, calculations at the B3LYP/6-31+G(d,p) level that include models for the substrate, Glu 165 and His 95 were carried out in the gas phase; calculations in which His 95 was replaced by a Gln residue were also performed. These gas-phase calculations (see Table A3 in Supporting Information) confirmed that His 95 has a destabilizing effect of around 5 kcal/mol. The unfavorable electrostatic interaction is not present when His 95 is replaced by a Gln residue, suggesting that path B is more likely to participate in the H95Q mutant.[5b,6a]

Interestingly, Alagona et al. found that, although the gas-phase intramolecular transfer has a barrier of 8.2 kcal/mol in a model system for EDT1 with a hydrogen atom replacing the methyl phosphate group, the barrier is reduced to 2.7 kcal/mol in the presence of the phosphate group (i.e., with the complete EDT1). From this result, even in the presence of destabilization by His95, path B would be expected to have the lowest activation barrier (see above). We have confirmed that the barrier for the intramolecular proton transfer is low (4.5 kcal/mol at the B3LYP/6-31+G(d,p) level) in the gas phase with the charged phosphate group. This is because the product EDT2 is strongly stabilized (by nearly 11.0 kcal/mol) by a hydrogen bond with the negatively charged phosphate group, so that the barrier for the proton transfer is reduced substantially in accord with the Hammond postulate. However, as shown in Table A4 in the Supporting Information, the barrier for the intramolecular proton transfer for the complete enediolate increases to 7.8 kcal/

(24) That the enediol along path A is not a shallow local minimum as found in ref 7 is due to the difference in the quantum mechanical levels. AM1, which was used in ref 7, gives too small a deprotonation energy for histidine and thus over-stabilizes the enzyme with the enediol in the active site.

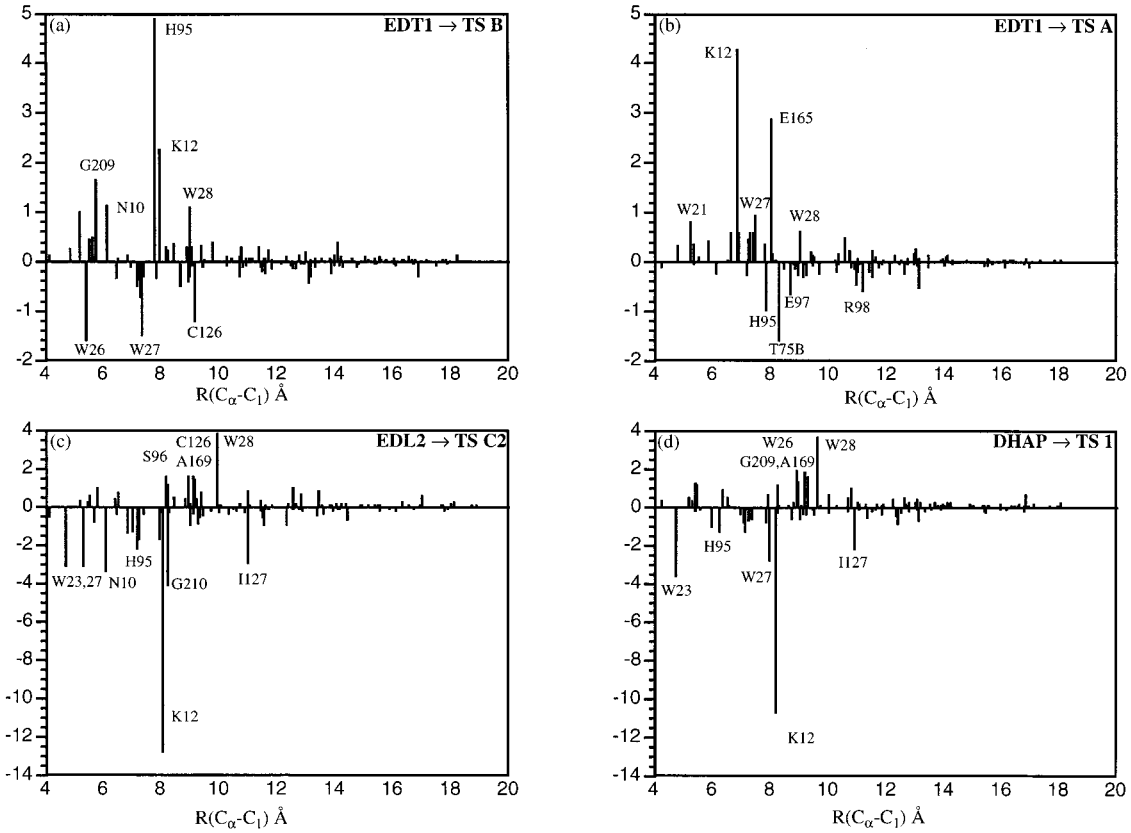

Figure 2. Perturbational analysis of electrostatic contributions at various stationary points (see Scheme 1) from the most important residues and water molecules (see text). As in ref 7, the contribution to a particular reaction process for each residue is defined as the energy difference caused by zeroing out the partial charges of this residue. A *negative* value indicates that the residue contributes favorably to a particular step of reaction. The difference in energy scale of the figures should be noted.

mol in the presence of solvent described with a continuum model; the value is similar to the results from models in which the phosphate group is substituted with a methyl group. Because the phosphate group is stabilized by charged and polar residues (e.g., Lys 12), as well as by water molecules (e.g., W23) in the enzyme active site, a better reference value for the intramolecular proton-transfer barrier is ~8 kcal/mol, rather than the value of 2.7 kcal/mol used in the analysis of Alagona.

For path A, Lys 12 and GluH 165 contribute to raising the barrier height for going from EDT1 to EDL1 because they favor EDT1 through electrostatic interactions (Figure 2b); a corresponding result was found in ref 7. One residue from the other subunit in the dimeric TIM, Thr 75B, is found to contribute to lowering the barrier height by about 2 kcal/mol through hydrogen-bonding interaction with His95. A similar effect has been observed by of Åqvist et al.,[9] although no quantitative results were given. The effect of Thr 75B can be related to the mutation results of Borchert and co-workers[23] that shortening the loop around Thr 75B yields a stable monomeric species that has a 1000-fold lower value of k_{cat}. The three residues (T75B, K12, and E165) together yield a value of 5.6 kcal/mol, relative to the total barrier of 8.0 kcal/mol; other significant residues are active-site water molecules W27 and W28, which contribute to raise the barrier, and H95 (mainchain), Glu97, and Arg98, which lower the barrier. Thus, the barrier for this step is actually increased in the enzyme, which is consistent with the fact that EDL1 is not stabilized; as suggested in ref 7 and confirmed in ref 4a, a neutral His 95 is involved in the proton transfer to avoid overstabilization of the enediol, EDL1. Since the increase in the barrier is due mainly to K12 and E165, the two residues that are critical for the first proton transfer (DHAP to E165), it is likely this is simply a (passive) consequence of the (active) stabilization of EDT1 by the enzyme. The major evolutionary pressure on TIM was to lower the barrier between DHAP and EDT1, in part by stabilizing the latter relative to DHAP (or GAP), since this corresponds to the slow step in the uncatalyzed reaction in solution.[26]

For path C, results for EDL2 → TSC2 are shown because this step has a higher barrier than EDT1 → TSC1. Lys 12 was found to make a large favorable contribution, because the substrate is more negatively charged in TSC2. A few other residues, including His 95, Asn 10, Gly 210, and two active-site water molecules (W23, W27) also favor the EDT2 over EDL2.

The common proton-transfer step from DHAP to EDT1 is the most difficult step in the uncatalyzed reactions in solution (endothermic by 23.4 kcal/mol according to model studies),[26] and therefore, the major function of TIM is to stabilize EDT1 and to lower the associated proton-transfer barrier. In agreement with previous theoretical studies,[7] Lys 12 has the dominant effect on the barrier: it lowers it by about 11 kcal/mol (see Figure 2d). Interestingly, a mutation study[27] showed that removal of Lys 12 abolished the catalytic power of TIM; however, the reason for this is that, in the absence of Lys 12, the substrate is not bound, so that the experiment gives no evidence concerning the catalytic role of Lys 12. The fact that Lys 12 has such a large polarization effect on the first proton transfer suggests that the *effective* dielectric constant in its region of the active site is

(25) Borchert, T. V.; Abagyan, R.; Jaenicke, R.; Wierenga, R. K. *Proc. Natl. Acad. Sci. U.S.A.* **1994**, *91*, 1515.
(26) Cui, Q.; Karplus, M. Manuscript in preparation.
(27) Straus, D.; Raines, R.; Kawashima, E.; Knowles, J. R.; Gilbert, W. *Proc. Natl. Acad. Sci. U.S.A.* **1985**, *82*, 2272.

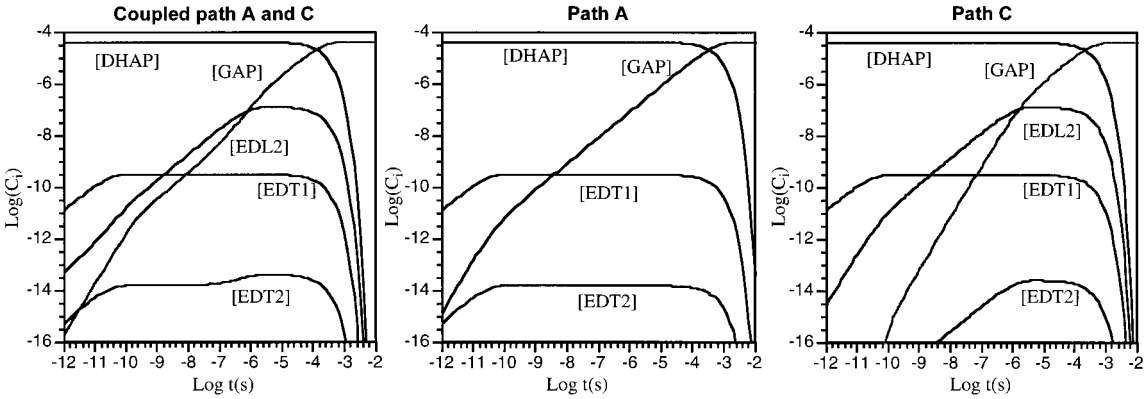

Figure 3. Concentration of a number of species (DHAP, EDL2, GAP) as a function of time according to the analytical solution of the coupled unimolecular proton-transfer reactions. The initial concentration of [DHAP] was set to 40 μM, the value used by Knowles and Albery.[2b,2d] Since the chemical steps are unimolecular, the choice of concentration makes no difference in the rates. We note that the calculated rate of disappearance of DHAP is 5.4×10^3 s^{-1}, as compared with the experimental value of 2×10^3 s^{-1}; this supports the use of kT/h as the preexponential factor and the value calculated for the activation free energy.

rather low. Two water molecules, W23 and W27, which are hydrogen-bonded to the phosphate group of the substrate and the main chain carbonyl of Glu 165, respectively, contribute substantially to stabilizing EDT1. There are some other residues that contribute favorably to the proton transfer (His 95, I 127, Gly 209, Ala 169; the latter three contribute through mainchain atoms. Two additional water molecules (W26, W28) make an unfavorable contribution. These results suggest that removing the three active-site water molecules (W26,27,28) would be likely to favor EDT1 over DHAP. This could explain the recent experimental results of Zhang et al.,[6c] who proposed that the absence of active-site water molecules (and a more hydrophobic environment that implies a better pK_a match between Glu 165 and the substrate) caused by the mutation S96P is the reason for the higher activity of the double mutant, E165D/S96P, compared to that of the single mutant, E165D;[6c] see also refs 8 and 28.

Kinetic Analysis. Because of the similarity in the calculated free energy barriers along paths A and C, kinetic modeling was performed to determine their relative contribution to the overall chemical reaction that transforms DHAP into GAP; path B was found to make a negligible contribution because of its high barrier and is not considered further. As shown in Figure 3, both paths A and C contribute significantly, with the former somewhat more important. However, the calculations are not sufficiently precise to distinguish between the two. The steady-state approximation was found to be valid for intermediates EDT1 and EDT2 along both paths A and C, as well as for EDL2 along path C. The apparent barriers for the disappearance of DHAP along path A and C are 13.0 (DHAP to TSA) and 12.7 kcal/mol (DHAP to TSC1), respectively; both are close to the experimental estimate of 13.0 kcal/mol.[2,29] The low tritium-transfer efficiency from the substrate to the product observed experimentally (i.e., that there is exchange of protons with the surrounding medium)[2,4c] could be due to exchange in the enediolate (paths A and C), or the enediol (path C). Along path C, the enediol species EDL2 accumulates on a microsecond time scale (Figure 3b, c), though the concentration remains small. The apparent barrier for the conversion from EDL2 to GAP along path C is 9.3 kcal/mol, somewhat lower than the experimental estimate of 11 kcal/mol.[2,29] It should be noted that the experimental barriers had to be obtained by a series of ingenious, but indirect, experiments based on isotope effects because the overall reaction is diffusion limited.[2] The activation free energies are estimated from the rates given in Figure 6 of ref 2d with the assumption of a preexponential factor of kT/h, equal to 6×10^{12} s^{-1} at 300 K. Although this is often too large for solution reactions,[29] it is likely to be approximately correct for the proton transfer. Moreover, the same preexponential factor appears to have been used in the analysis of refs 2b and d. An assumption in the kinetic model in ref 2c is that only *one* intermediate is involved in the chemical steps and this intermediate can undergo rapid proton exchange with the solvent. Along path A and C, both enediolate species (EDT1 and EDT2) can exchange a proton with the solvent, while along path C, the enediol (EDL2) can also undergo proton exchange. Whether the assumption made in ref 2c is valid depends on the rate constants associated with the possible mechanisms for proton exchange. There is not enough information to calculate how the free energy profile in ref 2c would change if more than one intermediate were involved in proton exchange. If one were to assume that only EDL2 can exchange protons with the solvent at a rate comparable to that in the catalytic steps, the experiments in ref 2 would suggest that path C is significant, given the calculated free energy profile.

Conclusions

Three mechanisms proposed for the triosephosphate isomerase (TIM)-catalyzed reactions were studied in a consistent manner with the QM/MM approach using B3LYP/6-31+G(d,p) as the QM method. The calculations indicate that the two paths that involve an enediol intermediate (that is, path A, originally proposed by Knowles et al.[1] and supported by the theoretical studies of Bash et al.[7] and Åqvist et al.,[9] and path C, which was originally proposed for the H95Q mutant[6c] and treated with theoretical models by Peräkylä et al.,[10]) make significant contributions to the TIM reaction. The calculation methods are not precise enough to determine which of the two is more important; in a recent analysis, Mildvan et al.[4c] found that both paths contribute but also were unable to determine their relative contributions. By contrast, the results appear to exclude the intramolecular pathway (path B) in the wild-type TIM, and model calculations suggest that this path might participate in the H95Q mutant. Since His 95 is essential for path A, plays a favorable role in path C, and inhibits path B, the conclusions from the present calculations are in accord with the fact that His 95 is conserved in all known TIM sequences.[3,6] Thus, the

(28) Joseph-McCarthy, D.; Petsko, G.; Karplus, M. *Protein Eng.* **1995**, *8*, 1103.
(29) Karplus, M. *J. Phys. Chem. B* **2000**, *104*, 11.

results provide important new information concerning the reaction mechanism of TIM, although certain questions remain to be resolved.[26]

Acknowledgment. Helpful discussions with Drs. X. Lopez, H. Guo, S. Fischer, and S.-S. So are gratefully acknowledged. We thank D. Arigoni for a stimulating discussion; his suggestion that the intramolecular proton transfer pathway was the "obvious one" was an element in our making the effort to revisit the TIM reaction. Part of the computations were done on the J90 machines at NERSC, SGI Origin2000 machines at NCSA, and the IBM SP2 machines at Argonne National Laboratory. The research was supported in part by the Department of Energy and the National Institutes of Health.

Supporting Information Available: Benchmark calculations at a number of QM levels (including B3LYP, MP2, and CCSD) for model species involved in TIM, values for the charge-scaling factors obtained from Poisson−Boltzmann calculations; results for a number of gas-phase models for the intramolecular proton transfer (path B) (PDF). This material is available free of charge via the Internet at http://pubs.acs.org.

JA002886C